View Article Online / Journal Homepage / Table of Contents for this issue

Production of arrays of chemically distinct nanolitre plugs *via* repeated splitting in microfluidic devices†

David N. Adamson, Debarshi Mustafi, John X. J. Zhang,‡ Bo Zheng§ and Rustem F. Ismagilov*

Received 6th April 2006, Accepted 20th June 2006
First published as an Advance Article on the web 27th July 2006
DOI: 10.1039/b604993a

Published on 27 July 2006. Downloaded by Dartmouth College on 30/07/2015 20:02:14.

This paper reports a method for the production of arrays of nanolitre plugs with distinct chemical compositions. One of the primary constraints on the use of plug-based microfluidics for large scale biological screening is the difficulty of fabricating arrays of chemically distinct plugs on the nanolitre scale. Here, using microfluidic devices with several T-junctions linked in series, a single input array of large (~320 nL) plugs was split to produce 16 output arrays of smaller (~20 nL) plugs; the composition and configuration of these arrays were identical to that of the input. This paper shows how the passive break-up of plugs in T-junction microchannel geometries can be used to produce a set of smaller-volume output arrays useful for chemical screening from a single large-volume array. A simple theoretical description is presented to describe splitting as a function of the Capillary number, the capillary pressure, the total pressure difference across the channel, and the geometric fluidic resistance. By accounting for these considerations, plug coalescence and plug–plug contamination can be eliminated from the splitting process and the symmetry of splitting can be preserved. Furthermore, single-outlet splitting devices were implemented with both valve- and volume-based methods for coordinating the release of output arrays. Arrays of plugs containing commercial sparse matrix screens were obtained from the presented splitting method and these arrays were used in protein crystallization trials. The techniques presented in this paper may facilitate the implementation of high-throughput chemical and biological screening.

Introduction

This paper describes methods for facilitating the production of arrays of nanolitre-sized plugs with distinct chemical compositions. The ability to react a single substance with a large set of reagents is important for a variety of applications including biological assays and protein crystallization trials.[1–6] The screening of a single reagent against arrays of distinct sub-microlitre plugs has been demonstrated.[3,4] Such plug-based high-throughput screening, however, requires methods to generate arrays of plugs with distinct chemical compositions with minimum labor and cost. 'Plugs' are defined as droplets, surrounded by carrier fluid, that block the channel but do not wet the walls. They are large enough to come in contact with the walls if it were not for a thin layer of carrier fluid wetting the surface.[7] Previously, we have demonstrated the production of arrays with plugs that are (a) chemically identical,[7] (b) alternating in composition,[8] and (c) changing in concentration of a certain reagent.[5] To create arrays where the composition of plugs is not constrained to periodic or graded patterns, solutions may be sequentially dispensed or aspirated into a capillary to produce individual arrays of droplets. This method is time consuming and small plugs (~20 nL) are difficult to accurately aspirate either manually or robotically. Arrays of larger sized plugs (~320 nL) are significantly easier to prepare.

Here we report a method that allows for the conversion of an array of large, distinct plugs into several arrays of smaller plugs of the same composition and configuration. We demonstrate this method by splitting[7,9] a single array of large (~320 nL) plugs *via* successive microfluidic T-junctions to produce 16 arrays of smaller (~20 nL) plugs (Fig. 1).

To implement successive splitting we characterized the following: (i) methods to preserve integrity of plugs by preventing coalescence of plugs during flow, preventing relative motion of plugs during flow, and preventing plug–plug contamination; (ii) methods to ensure symmetric splitting; (iii) device designs that allow for the preservation of plug extension; (iv) device designs that allow for the sequential release of output arrays through a single outlet.

Experimental

Fabrication of splitting devices

Microfluidic devices were fabricated using soft lithography in poly(dimethylsiloxane) (PDMS).[10] Microchannels were fabricated with rectangular cross sections using rapid prototyping.[11] This rapid prototyping method allows for micron order precision in the fabrication of channels along axes parallel to the plane of the device. The height of the microchannels,

5735 S. Ellis, University of Chicago, Department of Chemistry and Institute for Biophysical Dynamics, Chicago, IL, USA. E-mail: r-ismagilov@uchicago.edu; Fax: 773 702-0805; Tel: 773 702-5816

† Electronic supplementary information (ESI) available: AutoCAD designs of devices described in this paper. See DOI: 10.1039/b604993a

‡ Current address: 1 University Station, The University of Texas at Austin, Department of Biomedical Engineering, Austin, TX 78712, USA.

§ Current address: University Science Centre, The Chinese University of Hong Kong, Shatin, New Territories, China.

 This journal is © The Royal Society of Chemistry 2006

View Article Online

Published on 27 July 2006. Downloaded by Dartmouth College on 30/07/2015 20:02:14.

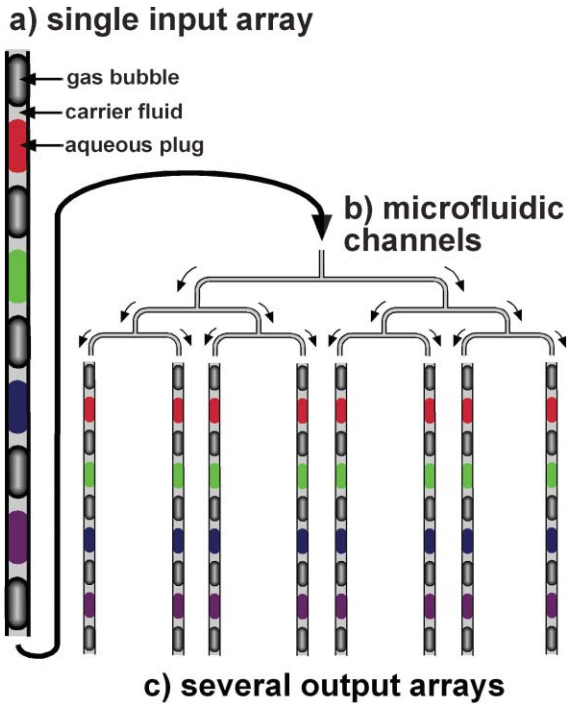

Fig. 1 A schematic drawing of the splitting process discussed in this paper. (a) A single input array is prepared with plugs of the screening solutions, arranged in the order desired in the output arrays. (b) The input array is injected into the splitting device; the plugs and gas bubbles in the array passively breakup at the T-junctions. (c) The smaller split plugs form several output arrays that can be used for chemical and biological screens and assays.

however, is more variable because it is determined by the thickness of the photoresist deposited on the silicon wafer used to form the template for the PDMS devices. Cross-sections of PDMS devices were taken and the actual channel dimensions were measured to determine how the actual dimensions varied from the designed values. Channel walls were functionalized with (tridecafluoro-1,1,2,2-tetrahydrooctyl)-1-trichlorosilane (United Chemical Technologies, Bristol PA) to minimize the adhesion of aqueous plugs to the channel walls.[10,12]

To simplify the fabrication process, only the widths of the microfluidic channels were varied across the device. For all single-outlet devices (16× and 4× splitters) and multiple-outlet devices (8×), the channel heights are ~250 μm and widths vary from ~50 to ~1000 μm. The inlet channels of each device begin ~1000 μm wide and taper gradually to the width of the first splitting junction. The outlet(s) of each device are ~250 μm by ~250 μm to accommodate the tubing used for collection of arrays. Specific channel widths within the device are given in the appropriate section.

Typical splitting experiment

All input arrays were aspirated into 30-gauge Teflon tubing (Weico Wire & Cable, Edgewood, NY) using a manual micro-syringe pump (Stoelting Company, Wood Dale IL) with glass syringes ranging in volume from 50 to 500 μL (Hamilton Company, Reno NV). The Teflon tubing and syringe were filled with fluorous carrier fluid specified for each experiment below. Each solution or gas in the array was then aspirated sequentially. In the Teflon tubing, plugs form spontaneously from the aqueous solution in the presence of the fluorous carrier fluid. Aspirated arrays generally contained ~20 plugs.

With the input array aspirated, the splitting devices were pre-filled with the carrier fluid used in the input array. The Teflon tubing containing the input array was sealed to the splitting device *via* the application and heat curing of PDMS. The arrays were propelled through the splitting device using a PHD 2000 syringe pump (Harvard Apparatus, Holliston MA). Output arrays were collected in thin Teflon tubing with O.D. ~230 μm and I.D. ~200 μm (Zeus, Raritan NJ).

Preventing the coalescence and relative motion of plugs during flow

For experiments testing relative motion and coalescence of plugs, two aqueous solutions were used in the input arrays. The viscous aqueous solution (V-A1) was 0.07 M $Fe(SCN)_x^{3-x}$ in 68% glycerol in water (red) and the non-viscous aqueous (NV-A1) solution was 1.0 M $CuSO_4$ in water (light blue). A mixture of 1H,1H,2H,2H-perfluorooctanol (PFO, from Alfa Aesar) (1 : 10 v/v) and FC-3283 (3 M Fluids) was used as the carrier fluid. The first input array was generated by aspirating ~320 nL of V-A1 in alternation with ~320 nL of the carrier fluid. The second input array was generated by aspirating ~320 nL of each solution in the following repeated pattern: V-A1, carrier fluid, NV-A1, carrier fluid. The third input array was generated by aspirating ~320 nL of each array component in the following repeated pattern: air, V-A1, air, carrier fluid, air, NV-A1, air, carrier fluid. The channel dimensions for this experiment were 800 μm (width) by 200 μm (height). The flow rate through the channel shown was 50 μL min^{-1}.

Preventing plug–plug contamination

For the experiments that revealed plug–plug contamination, Hampton Crystal Screen I solutions 1–16 (Hampton Research, Aliso Viejo CA) were aspirated in ~160 nL volumes in alternation with air to form the input array. These Hampton Crystal Screen solutions ranged in viscosity from ~1 mPa s to ~50 mPa s.[13]

To ensure that plug–plug contamination can be reliably prevented, splitting trials were conducted with arrays of nine plugs. The plugs in the center of the arrays were labeled with fluorescein (Molecular Probes) at a very high concentration (1/20 of saturation at room temperature); the other plugs in the array were unlabeled. Fluorescence measurements (Leica DM IRB with Spot Insight QE camera) were taken of both the input array prior to splitting and the 16 output arrays. Only the splitting descendents of the originally labeled plug produced detectable fluorescence signals at maximum gain. For these plug–plug contamination experiments, two aqueous solutions were used. The viscous aqueous solution (V-A2) was glycerol in water (76% w/w, viscosity ~40 mPa s) and the non-viscous aqueous (NV-A2) fluid was water (viscosity ~1 mPa s). A mixture of PFO (1 : 10 v/v) and FC-3283 was used as the carrier fluid. The input arrays used for these experiments were generated by repeatedly aspirating ~320 nL of each of array component in the following repeated pattern: air, V-A2, air,

View Article Online

Published on 27 July 2006. Downloaded by Dartmouth College on 30/07/2015 20:02:14.

NV-A2. Separate experiments were conducted with the fluorescein solution in V-A2 and NV-A2 plugs.

Characterization of the symmetry of splitting in devices with multiple T-junctions

For the characterization of splitting consistency, two aqueous solutions were used (V-A2 and NV-A2 as defined in the previous section). PFO (1 : 10 v/v) in FC-3283 was used as the carrier fluid. Input arrays were generated by repeatedly aspirating ~320 nL of each of array component in the following repeated pattern: air, V-A2, air, NV-A2. Splitting consistency experiments were conducted using splitting devices with geometries reflecting design strategies (a) and (b) (Fig. 6) and with injection flow rates of 16, 40 and 160 μL min^{-1}.

For the 16× splitting device (a), all four splitting junctions and the channels connecting them had width 120 μm. The array storage channels following the splitting region also had width 120 μm. For the 16× splitting device (b), the splitting junctions had widths ~425, ~213, ~107 and ~53 μm and the regions immediately following each T-junction had widths ~453, ~320, ~226 and ~160 μm. The array storage channels following the splitting region had width 120 μm. The compressible region of the output channels had width 200 μm.

In the measurement of splitting consistency, each split plug contributes a single data point to the splitting consistency distribution. The location of that data point is given by the percent difference between the length (and thus the volume) of the split plug and the average of the lengths of the other plugs formed from the splitting of the same input plug (Fig. 5). Plug length data was acquired from digital images taken with a Canon EOS Digital Rebel XT with a 180 mm EF Canon Macro Lens. Images were taken of all output arrays simultaneously. For experiments with an injection flow rate of 40 μL min^{-1} or higher, each output plug's corresponding input plug was identified based on its position in its output array. For experiments with an injection flow rate of 16 μL min^{-1}, a time series of images was taken so the origin of each plug in the output arrays could be determined by tracing each plug during splitting.

To address the contribution of the variation in channel dimension on the consistency of splitting, slices of devices of types (a) and (b) were taken and measurements of the dimensions of the output channel sizes were recorded. From 96 channel measurements, the variability of the width and height of the channels is approximately 4 and 10% of the mean respectively (one standard deviation). Combined, the variability in the channel dimensions can induce a channel-to-channel variability in volumetric flow rate of ~20% (one standard deviation). This variability in channel size explains, at least in part the baseline variability in the plug volume that exists even when the single-phase flow approximation holds (Fig. 5).

Coordinated release of split arrays: valve-based system

To form the input array used in tests of the valve-based release system, Hampton Crystal Screen I solutions 1–12 were aspirated in ~320 nL volumes in alternation with air. These solutions ranged in viscosity from ~1 to ~20 mPa s. A mixture of PFO (1 : 10 v/v) and FC-3283 was used as the carrier fluid.

Splitting devices requiring valves were fabricated with microfluidic channels set ~1 mm from the surface of the device. Output channels with dimensions 250 μm tall by 200 μm wide were aligned above threaded holes in a bronze plate to allow for the use of machine screws (5/64 inch) to compress the channels. The volume displaced by the valve is on the order of 100 nL. Other channel dimensions were as the 16× splitting device (b) above. The aligned splitting devices were clamped between the bronze plate and a layer of translucent plastic to allow for visualization of the devices. Eight of the 16 output channels of a four-level splitting device were equipped with these compression valves. An injection flow rate of 400 μL min^{-1} was used for splitting. The injection flow rate was then reduced to ~1 μL min^{-1} for the release of the output arrays. The contents of each of the eight output channels were released from the device in sequence *via* selective compression of the output channels.

Coordinated release of split arrays: volume-based system

Throughout this paper, we use the term "geometric fluidic resistance" R_g [m^{-3}] to refer to the component of the fluidic resistance determined only by the geometry of the channel in single-phase flow. The geometric fluidic resistance is given by $R_g = \Delta P/(U_v\mu)$ where ΔP [Pa] is the pressure difference across the channel, U_v [m^3 s^{-1}] is the volumetric flow rate of fluid through the channel and μ [Pa s] is the dynamic viscosity of the (single-phase) fluid in the channel. For flow involving multiple phases, the geometric fluidic resistance becomes more complicated due to the presence of interfaces. The linear relationship between the pressure difference and the volumetric flow rate for a given fluid stream does not hold for these systems. In these situations we will still refer to "geometric fluidic resistance," but we will be referring to the geometric fluidic resistance as determined for a single-phase flow where physical properties of the carrier fluid are used for the single continuous phase.

The pressure drop associated with a single-phase fluid passing through a microfluidic channel with a rectangular cross-section is given by $\Delta P = \{24[1 - 1.3553\alpha + 1.9467\alpha^2 - 1.7012\alpha^3 + 0.9564\alpha^4 - 0.2573\alpha^5]U_mL\mu[1 + a/b]^2\}/8a^2$ where ΔP [Pa] represents the pressure drop, α [unitless] represents the aspect ratio of the channel ranging from 0 to 1, U_m [m s^{-1}] represents the average flow rate though the channel, L [m] represents the length of the channel, μ [Pa s] represents the dynamic viscosity of the fluid and a, b [m] represent the half-width and half-height of the channel respectively.[14] The geometric fluidic resistance is thus $R_g = \{6[1 - 1.3553\alpha + 1.9467\alpha^2 - 1.7012\alpha^3 + 0.9564\alpha^4 - 0.2573\alpha^5]L[1 + a/b]^2\}/8a^3b$.

To form the input arrays used in tests of the volume-based release system, Hampton Crystal Screen I solutions 1–10 were aspirated in ~80 nL volumes in alternation with air. FC-3283 or a mixture of PFO (1 : 5 v/v) and FC-3283 was used as the carrier fluid. Injection flow rates ranged from 30 to 100 μL min^{-1} for splitting and from 1 to 40 μL min^{-1} for the release of output arrays.

For the 4× volume-based splitting device, the splitting junctions had widths ~107 and ~53 μm and the regions

 This journal is © The Royal Society of Chemistry 2006

View Article Online

Published on 27 July 2006. Downloaded by Dartmouth College on 30/07/2015 20:02:14.

immediately following each T-junction had widths ~226 and ~160 μm. The array storage channels following the splitting region had width 120 μm. Following the splitting and array storage regions of the device, each of the four output channels were designed with distinct geometries. The geometric fluidic resistances of these channels were identical although each channel had a distinct volume. Channel widths for channels 1, 2, 3 and 4 were 100, 124, 145 and 163 μm, respectively. The lengths of these channels were 100 000, 154 360, 211 820 and 269 320 μm, respectively.

Splitting arrays of plugs of Hampton crystal screen solutions

Hampton Crystal Screen I solutions 1–25 were aspirated in one input array, and solutions 26–50 were aspirated in a second input array. Approximately 320 nL volumes of the solutions were aspirated in alternation with air. Two different experiments were done with FC-3283 and a mixture of PFO (1 : 10 v/v) with FC-3283 as the carrier fluids. The injection flow rate used for splitting was 160 μL min^{-1}. Measurements of splitting symmetry were taken as described in "Characterization of the symmetry of splitting in devices with multiple T-junctions" above.

Results and discussion

Preventing plug coalescence during flow

During flow, plugs with different chemical composition may move relative to the carrier fluid at different rates and thus move relative to one another allowing adjacent plugs to coalesce (Fig. 2(b)). Coalescence presents two problems: (1) it prevents either of the reagents present in the merged plugs from being used separately, defeating the purpose of the chemical screen and (2) it complicates the process of identifying reagents by their location in the array. The motion of plugs relative to a carrier fluid has been characterized as a function of several parameters, including the Capillary number, the viscosity ratio between the plug and the carrier fluid,[15] the surface tension between the plug and the carrier fluid, the density of the plug, the concentration of surfactant at the plug/carrier fluid interface, and the surfactants sorption kinetics.[16] The Capillary number, Ca, is a dimensionless ratio of viscous forces to surface tension forces and is defined by $Ca = U\mu/\gamma$, where U [m s^{-1}] is the rate of flow, μ [Pa s^{-1}] is the viscosity of the fluid, and γ [N m^{-1}] is the surface tension. It has been shown that as the viscosity of the droplet or plug is increased relative to that of the carrier fluid, the velocity of that droplet will decrease relative to the average velocity through the channel.[15] This change in relative motion is closely correlated with the gap between the droplet and the channel wall; the higher the velocity of the plugs relative to the average velocity through the channel, the greater the gap between the droplet and the channel wall.[15] In agreement with these observations, when an array of plugs of significantly differing viscosities (~1 *vs.* ~18 mPa s) was flowed through a microfluidic channel, coalescence was observed after the array had traveled less than 2 cm in the device (Fig. 2(b)(ii)). When an array of chemically identical plugs was flowed through the same channel under the same conditions, no observable relative motion was observed even after the array had traveled ~20 cm (Fig. 2(a)).

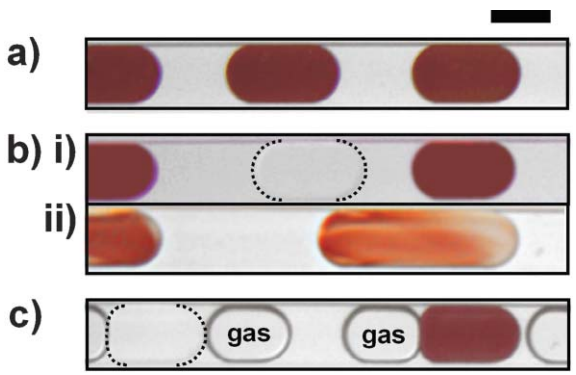

Fig. 2 Images of arrays of plugs in microfluidic channels during flow showing relative motion and coalescence of plugs (see Experimental section for details). (a) Plugs with identical chemical composition (and thus, with identical physical properties) did not move relative to one anther significantly during flow. Plugs were all of viscous solutions. (b) Plugs of distinct chemical composition (i) moved relative to one another during flow and eventually (ii) coalesced. Plugs are alternating viscous (red) and non-viscous (light blue) solutions. (c) The placement of air bubbles between plugs of distinct composition retarded their relative motion and prevented coalescence. The direction of flow is left-to-right and the carrier fluid is FC-3283 10 : 1 PFO (v/v) throughout. The scale bar is ~800 μm.

To prevent coalescence, gas bubbles can be introduced as spacers between plugs to (1) minimize the relative motion of plugs and (2) to act as a physical barrier to prevent the coalescence of adjacent plugs during flow and splitting. Three-phase flow with gas bubbles placed between aqueous droplets in a carrier fluid has been proposed and demonstrated previously.[16] This three-phase flow has also been used with microfluidic-based chemical screens to prevent the coalescence of plugs during flow.[4] During splitting, this three-phase flow configuration prevented adjacent plugs of distinct composition from coalescing (Fig. 2(c)). Using these spacers, we split arrays of plugs of solutions with dissimilar viscosity, surface tension, and density. The viscosity of our solutions ranged from ~1 to ~60 mPa s, the surface tensions were ~10–12 mN m^{-1} and the densities fell between 1.0 and 1.3 g mL^{-1}.

Preventing the relative motion of plugs during flow

The relative motion of plugs during flow and splitting can change the distances between adjacent plugs and compromise the usability of output arrays because some screening methods rely upon a regular spacing between adjacent plugs.[4] If the initial arrays are configured such that the gas bubbles are in contact with both adjacent plugs, then the net accumulation or removal of carrier fluid between the plugs of the array is minimized. In situations where gas bubbles can transmit the contents of one plug to another (*i.e.* the transmission of water *via* osmotic pressure), carrier fluid can be inserted between the plugs and the gas bubbles of the array after splitting has occurred.

View Article Online

Published on 27 July 2006. Downloaded by Dartmouth College on 30/07/2015 20:02:14.

Preventing plug–plug contamination

Even with the use of gas spacers as discussed above, undesired contamination of one plug by the contents of another can still occur. We have observed that small droplets have the capacity to move past gas bubbles in three-phase flow by traveling between the air bubble and the wall of the channel. If plugs are allowed to break up into these smaller droplets, adjacent plugs could contaminate one another despite the presence of gas spacers. It is well known that flows with higher Capillary number can induce plugs to break up while those with lower *Ca* do not.[17–19] It is possible then, that at high Capillary numbers, we will observe plug–plug cross contamination while at low Capillary numbers, we will not.

In agreement with this interpretation, we have observed that when splitting trials are conducted with a high viscosity carrier fluid (PPP 10 : 1 PFO (v/v), viscosity ~18 mPa s), cross-reactions between the adjacent plugs of solutions of Hampton Crystal Screen I (14, 15 and 16), were observed in every output array. When the carrier fluid was changed to one of lower viscosity (FC-3283, 10 : 1 (v/v) PFO, viscosity ~1 mPa s) no cross reactions were observed. This decrease in viscosity represents an 18-fold decrease in the Capillary number from ~0.18 to ~0.01 (calculated from the carrier fluid viscosity with channel dimensions 53 μm by 250 μm corresponding to the highest Capillary number along the path of flow). In short, this section establishes the importance of maintaining a low Capillary number during flow to prevent spontaneous breakup of plugs and subsequent plug–plug cross contamination (Fig. 3).

It is probable that channels with circular (rather than rectangular) cross sections would inhibit the movement of small aqueous droplets past gas spacers because the spacers would more effectively block a circular channel, but this hypothesis has not been tested.

Controlling the symmetry of splitting in multiple T-junction splitting devices

The controlled splitting of plugs *via* a single T-junction microchannel geometry has been demonstrated[7] and is well characterized.[9] The Capillary number and plug extension at the splitting junction determine whether or not aqueous plugs will split at T-junctions, while the relative pressure differences across the two outlet channels determines the relative size of the resulting plugs. Plug extension ε [unitless] is defined by $\varepsilon = l/\pi w$ where l [m] and w [m] are the length and width of the plug in the T-junction, immediately after it vacates the junction's incident arm (trunk of the letter 'T').[9]

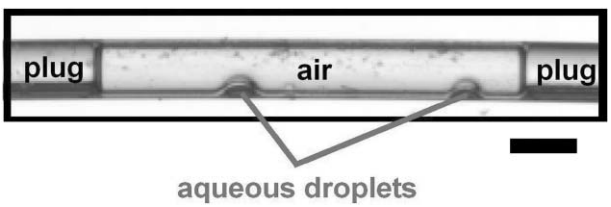

Fig. 3 The spontaneous breakup of plugs in three-phase flow can produce small droplets capable of moving past gas bubble spacers. These smaller droplets can then merge with adjacent plugs, causing plug–plug contamination. The intermediate state shown above with small aqueous droplets trapped between the tubing wall and an air bubble spacer was observed after splitting. The splitting trial was conducted with Hampton screen plugs 1–16; FC-3283 10 : 1 PFO (v/v) was used as the carrier fluid. The plugs are displayed within a thin segment of Teflon tubing with circular cross section external to the splitting device. The scale bar is ~250 μm.

The symmetric splitting of a plug through a T-junction requires that the pressure differences across the two output channels be equal. This requirement is easily accomplished in a device that contains only a single T-junction because the pressure differences across each of the output channels are controlled primarily by the geometry of those channels. In contrast, when several T-junctions are linked together with the outputs of one leading into the inputs of two others, we have repeatedly observed highly asymmetric splitting despite the equality of the geometric fluidic resistance across the output channels. We believe that this asymmetry is the result of capillary backpressure generated as plugs and gas bubbles enter and are split by downstream T-junctions.

Capillary backpressure is generated when a plug or a gas bubble is split through a T-junction because a force will be generated by the aqueous/carrier fluid or gas/carrier fluid interface as it resists an increase in its area.[20] This backpressure can be quantitatively described by the Young–Laplace equation, $\Delta P_{YL} = \gamma(dA/dV)$, which gives the pressure difference ΔP [Pa] between the interior and exterior of a droplet (or plug) in terms of the surface tension γ [N m^{-1}] and a term determined by the geometry of the plug (dA/dV) [m^{-1}]. Because the flow is quasi-periodic, the backpressure generated by each T-junction will fluctuate in time as each plug reaches it and is split. This implies that if plugs enter downstream T-junctions at times that are not precisely coordinated, the pressure drops across the two exiting arms of the upstream T-junctions will not be balanced. This time dependent imbalance will cause a corresponding disparity in flow rate between outbound branches of upstream junctions (Fig. 4(b)). In turn, the difference in flow rates will produce irregularities in the volume of the plugs in the output arrays. Once this disparity in flow rates has been generated, the thin layer of lubricating carrier fluid can drain from between the slow moving plugs and the channel wall, especially at areas of roughness at the wall. This effect makes it more difficult to accelerate flows once they have stopped and plugs have pinned at the wall, further amplifying the splitting asymmetry.

If this interpretation is correct, it should be possible to reduce the asymmetry of splitting by minimizing the discrepancy between the total pressure difference across the two exiting arms of a T-junction. For this discussion, we approximate the total pressure difference across the channel by writing it as the sum of two terms, (1) the pressure difference that would exist in the channel assuming the same conditions with a single-phase fluid stream and (2) a perturbation representing the additional backpressure generated by the interfacial forces: $\Delta P_{total} = \Delta P_{single\text{-}phase} + \Delta P_{interface}$. Since the splitting backpressure from downstream T-junctions is responsible for the difference in the pressure drop between the exiting arms of upstream T-junctions, we should be able to minimize this relative difference by decreasing the splitting backpressure

 This journal is © The Royal Society of Chemistry 2006

View Article Online

Published on 27 July 2006. Downloaded by Dartmouth College on 30/07/2015 20:02:14.

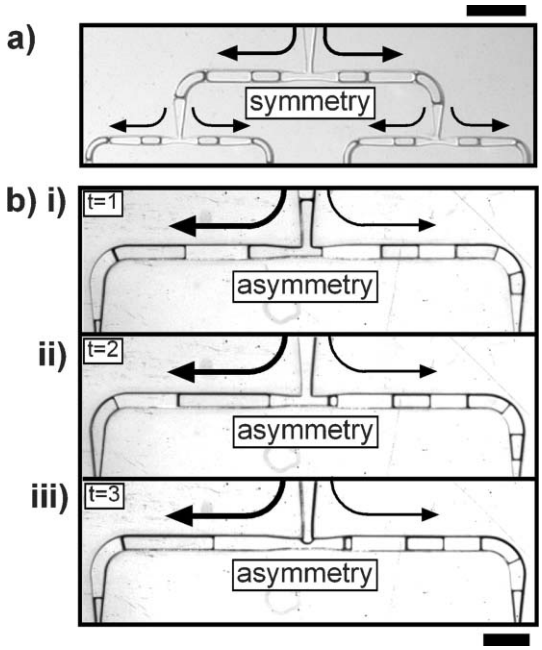

Fig. 4 (a) When the pressure differences across two splitting arms are equal, splitting is symmetric at the upstream T-junction closest to these arms. A single still image of symmetric splitting is shown. Injection flow rate was 160 μL min^{-1}; plugs alternated V-A2 and NV-A2 in FC-3283 10 : 1 PFO (v/v); junctions 2.2, 3.3 and 3.4 shown (Fig. 6). (b) When the pressure differences across the two splitting arms are unequal due to capillary backpressure, the symmetry of splitting at the upstream T-junction may be disrupted. (i)–(iii) Three sequential images illustrating asymmetric splitting are shown. Injection flow rate was 16 μL min^{-1}; plugs alternated V-A2 and NV-A2 in FC-3282 10 : 1 PFO (v/v); junction 1.1 shown (Fig. 6). Both scale bars are ~800 μm. Solution abbreviations are given in the Experimental section.

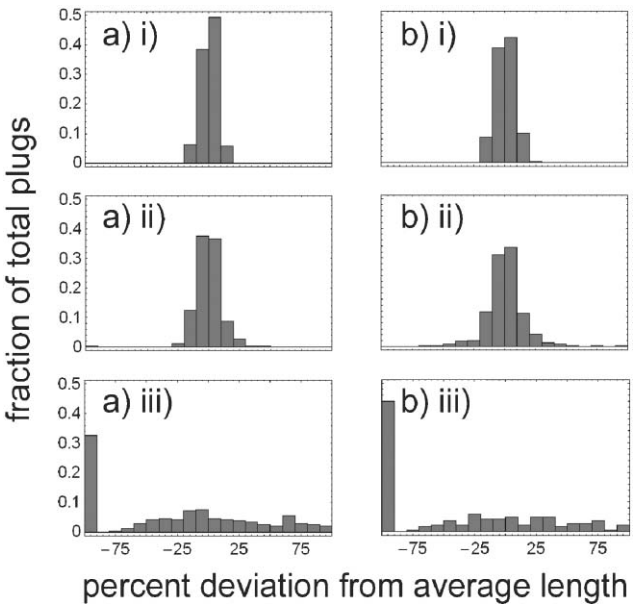

Fig. 5 The symmetry of splitting as measured by the variability in output plug size (see Experimental section). (a) Splitting symmetry measurements for device design 'a' (design shown in Fig. 6(a)) (b) Splitting symmetry measurements for device design 'b' (design shown in Fig. 6(b)). For both (a) and (b), images (i)–(iii) represent measurements for injection flow rates 160, 40 and 16 μL min^{-1}, respectively. The symmetry of splitting increases at higher volumetric flow rate as predicted by the theoretical arguments presented in the text. The difference in splitting symmetry between device 'a' and 'b' is small.

relative to the total pressure drop: $\Delta P_{total} \gg \Delta P_{interface}$. This can be accomplished by ensuring that $\Delta P_{single\text{-}phase} \gg \Delta P_{interface}$. To make this equation more meaningful in terms of experimental parameters, we relate $\Delta P_{interface}$ with the pressure difference given by the Young–Laplace equation ($\Delta P_{interface} \propto \Delta P_{YL}$) and equate $\Delta P_{single\text{-}phase}$ with the pressure difference given by the equation in the experimental section for single-phase flow in channels with rectangular cross section ($\Delta P_{single\text{-}phase} = \Delta P_{RCS}$). Systems where the pressures generated by interfacial phenomena are small relative to the total pressure drop are referred to as being in the ''single-phase flow approximation'' regime.

This formulation of the relationship between $\Delta P_{interface}$ and $\Delta P_{single\text{-}phase}$ predicts that if we tune the physical parameters of the system to increase the flow induced pressure drop relative to the interfacial pressure given by the Young–Laplace equation, we should be able to increase splitting symmetry. Indeed, Fig. 5 quantitatively compares the consistency of plug size in the output arrays as it was affected by splitting symmetry at different flow rates. As predicted, there is a marked decrease in the asymmetry of splitting with this 10-fold increase in flow rate. In addition, comparisons between splitting experiments using carrier fluids with surfactants and those without show that splitting is more regular when surface tensions are kept low (*i.e.* $\gamma \sim 10$ mN m^{-1} *vs.* $\gamma \sim 50$ mN m^{-1}), also in agreement with the predictions above. In all experiments conducted, more symmetric splitting was achieved when the physical parameters of the array were adjusted to increase the total pressure drop relative to interface-related pressure. In short, this section establishes that to maintain symmetric splitting it is important to maintain $\Delta P_{single\text{-}phase} \gg \Delta P_{interface}$, where $\Delta P_{single\text{-}phase}$ is given by the equation that describes the flow induced pressure drop (which depends on the channel cross section used) and $\Delta P_{interface}$ is proportional to the Young–Laplace equation.

Designing devices that promote splitting symmetry without promoting the spontaneous breakup of plugs

In the previous section we have shown that large pressure gradients are required for symmetric splitting. In the section before, however, we established the importance of maintaining a low Capillary number during flow to prevent spontaneous breakup of plugs and subsequent plug–plug cross contamination. Thus to ensure viable splitting over a wide range of flow parameters, it is important to maximize parameters of the system that increase $\Delta P_{single\text{-}phase}$ relative to $\Delta P_{interface}$ without also increasing the Capillary number. This goal can be accomplished *via* several methods including the use of (1) long microchannels (as was done with our devices) or (2) downstream regulator valves. Decreasing cross sectional dimensions of the channel can increase $\Delta P_{single\text{-}phase}$ relative to $\Delta P_{interface}$ as well. Unfortunately, for a given volumetric flow rate, this change also increases the *Ca* of the system.

View Article Online

Published on 27 July 2006. Downloaded by Dartmouth College on 30/07/2015 20:02:14.

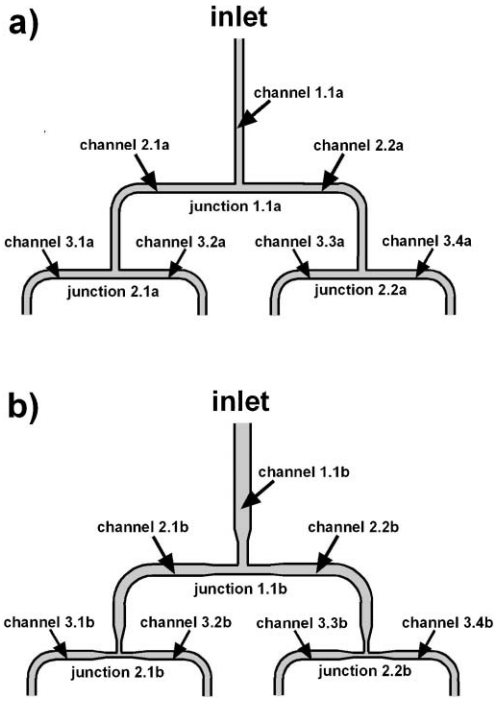

Fig. 6 Two design strategies used for the splitting regions of the microfluidic splitting devices. (a) Designs with channels with unchanging cross section dimensions allow for more symmetric splitting but also require that plugs take on large plug extension values near the inlet. (b) Designs with channels with decreasing cross section dimensions can maintain the extension of plugs. Changing the cross section dimensions, however, can induce additional capillary backpressure further disrupting the symmetry of splitting.

Designing splitting devices with multiple T-junctions

Here, two strategies for the design of successive T-junction devices are presented (Fig. 6). In the first (Fig. 6(a)), the dimensions of the microfluidic channels at and between each of the T-junctions are maintained throughout the splitting region.[9] While this design is easy to implement, the extension of plugs near the inlet of the device is several times greater than that of split plugs. Plugs with large plug extension values may spontaneously breakup in channels, destroying the integrity of the splitting process and the configuration of the output arrays. This discrepancy in plug extension increases exponentially with the number of splitting levels in the device, so while problems associated with spontaneous plug breakup may be minimal for splitting devices that only make use of 3–4 levels of T-junctions, this design may prove difficult to use for devices with additional splitting levels.

To minimize the discrepancy in plug extension, device design (b) is used (Fig. 6(b)).[7] With this design strategy, the dimensions of the channel decrease as the arrays are split further. Reducing the cross section area of the channels between splitting junctions by a factor of $2^{1/2}$ preserves plug extension in those regions. In addition, reducing the cross section area of the splitting junctions by a factor of two after each successive split preserves the Capillary number at each splitting junction.

One anticipated disadvantage of this second design arises from the constriction of channels between successive T-junctions. Plugs increase their surface area when flowing through channel constrictions and thus there is an additional backpressure that resists such a flow. With more sources for backpressure, there exist more opportunities for splitting inconsistency. While device design (a) in theory should produce more symmetric splitting, we found that the difference in the symmetry of splitting between devices that use strategy (a) *vs.* strategy (b) is small (Fig. 5). In either of the above cases, the flow rate and factors that influence the "single-phase flow" pressure drop are more significant than the differences between the two presented design strategies.

In short, when the Capillary number associated with the flow of individual plugs is low enough to prevent spontaneous breakup device design (a) is preferable. When it becomes difficult to balance this requirement for low Capillary number with the need to increase the total pressure drop across splitting junctions, device design (b) can reduce the *Ca* requirements to prevent spontaneous plug breakup without requiring a particularly large sacrifice in splitting symmetry. For the scenarios we have explored here, either design strategy will operate effectively.

Coordinated release of output arrays

With the device described so far, once the initial array has been split, each array is contained within the device in a separate channel and is released from the device *via* a separate outlet for storage or immediate use. For certain applications it may be useful for each array to exit the device *via* these separate channels (*i.e.* if the split arrays are to be used in several different experiments in parallel and thus each output is to be connected to another separate microfluidic device). Single-outlet splitting devices, however, provide a number of practical advantages over multiple-outlet devices. First, when each of the output channels of a splitting device is linked to a separate outlet, it can be more difficult to ensure that the pressure difference across these channels remains the same, making the preservation of splitting symmetry more difficult. Many sources of pressure fluctuation, are eliminated in single-outlet devices. Second, the post splitting manipulation of arrays (*i.e.* the insertion and removal of carrier fluid spacers) is more easily completed if it can be done at a single outlet several times rather than at several outlets once. Third, single outlet devices facilitate the joining of screening or other experiment-platform devices directly to a splitting device. If each of the arrays is to be used immediately for several experiments that require the same microfluidic device only one of those downstream devices would be needed. Here we present implementations of two different systems for the coordinated release of output arrays.

Active valve-based release systems. Sequential release of each of the output arrays can be accomplished with the use of valves (Fig. 7(a)). Several established techniques exist for fabricating and operating microfluidic valves.[21,22] Any of these technologies could be used to control the release of output arrays. Using one of these systems,[22] valves capable of selectively compressing portions of individual PDMS output channels were installed on splitting devices. Compressing the portion of

 This journal is © The Royal Society of Chemistry 2006

View Article Online

Published on 27 July 2006. Downloaded by Dartmouth College on 30/07/2015 20:02:14.

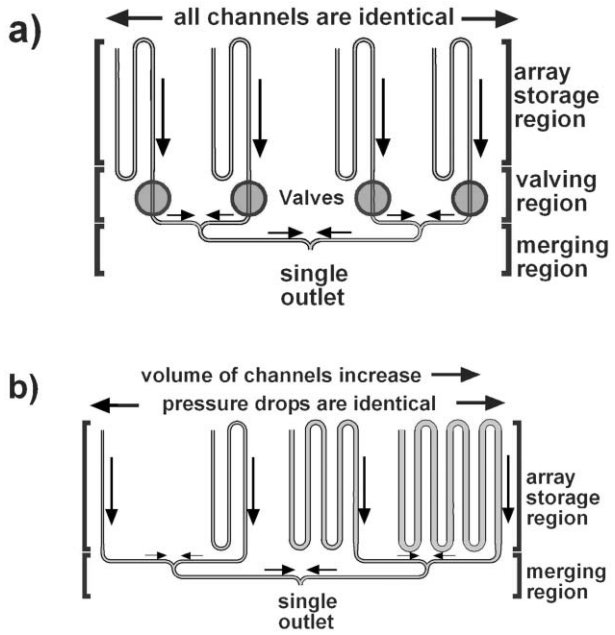

Fig. 7 Two methods for coordinating the release of arrays through a single outlet. (a) Valves that constrict the microfluidic channels individually can be used to prevent flow from all but one output channel at once. This system can be used to release the output arrays sequentially. (b) A set of channel geometries can be devised with identical pressure differences (in the single-phase flow limit) and distinct volumes. In the single-phase flow regime, the volumetric flow rate through these channels will be equal, and arrays can be passively released sequentially from the splitting device.

the channels between the array storage region and the single device outlet was enough to selectively restrict the flow of individual output arrays and release them sequentially.

Passive volume-based release systems. As an alternative to the valve-based release system, it is possible to use a passive, volume-based release system to coordinate the release of the output arrays. This can be implemented by selecting the appropriate geometry for the channels connecting the splitting region of the device to the outlets. Output channels were designed with identical geometric fluidic resistances. In the ideal case of single-phase flow, this allows for the preservation the volumetric flow rate through each channel, eliminating splitting bias. In contrast to other devices, however, the volume of each of the output channels was designed to differ from one another in increments of at least 1.5 times the expected volume of split arrays ($\sim$1 μL). Since each output channel has a distinct volume and the volumetric flow rate through each channel is identical, the contents of each output array will reach the outlet at a different time, allowing for sequential release of the output arrays.

The design of channels with identical geometric fluidic resistances and distinct volumes was accomplished by adjusting the width and length of each channel (Fig. 7(b)). Channels with small cross-section dimensions can produce a large geometric fluidic resistance over a short distance (far left of Fig. 7(b)) while wider channels require a greater length to achieve that same resistance (far right of Fig. 7(b)).

In splitting experiments where we used these volume-based splitting devices, each array exited the device separately as long as surfactant was present in the carrier fluid. In cases where surfactant was not included, the contents of the widest channel was observed to exit the device first, indicating a significant increase in the volumetric flow rate of that channel relative to the others. This and other experiments are consistent with the interpretation that a capillary backpressure resisting flow is generated by the plugs in the array that increases as the plugs are distorted by the confines of the channel.

Selection of an appropriate release system. With the use of volume-based splitting devices, a significant volume of carrier fluid is inserted between each pair of plugs when the array exits. Often these spacers of carrier fluid are much longer than is convenient for conducting chemical screens. It is possible to remove or reduce this volume of carrier fluid from between adjacent plugs and gas bubbles[6,23,24] but this method may complicate the use of the device. If the presence of a large volume of carrier fluid between plugs in the output array is not a concern, the simplicity of operation of the volume-base splitting design makes it the most attractive method for releasing output arrays sequentially. If, however, the distance between plugs needs to be kept small and consistent, valve-based splitting is the preferred option.

Conclusions

In this paper, we have described and experimentally characterized five criteria for reliable repeated splitting of arrays of plugs. First, to avoid instabilities leading to asymmetric splitting, the contribution of interfacial pressures to the total pressure difference across the arms of splitting junction has to be minimized. Second, to avoid spontaneous plug breakup and plug–plug contamination the Capillary number for the flow through the splitting device must be maintained below a critical value. The operating regime where these two criteria are satisfied can be widened by the use of splitting devices containing long output channels, as these channels increase the geometric fluidic resistance without also increasing the *Ca.* Third, to prevent coalescence of plugs of solutions with different physical properties, such plugs should be separated with gas spacers. Fourth, for devices that split arrays with a large number of serially connected T-junctions, it may be necessary to use channels that maintain plug extension during flow; the use of this design does not significantly disrupt the symmetry of splitting. Fifth, for applications where it is desirable to collect output arrays *via* a single device outlet, valve-based or volume-based methods of array release can be used.

We successfully used this method to split arrays of a commercially available sparse matrix protein crystallization kit from Hampton Research (Crystal Screen I). The sparse matrix kit contained solutions with viscosities ranging from $\sim$1 to $\sim$50 mPa s.[13] The consistency of splitting of arrays of the Hampton Screen kit was in agreement with the data obtained in Fig. 5. Output arrays of this crystal screen obtained from splitting were used to set-up sparse matrix protein crystallization trials.[4] Several proteins with unsolved structures,

View Article Online

Published on 27 July 2006. Downloaded by Dartmouth College on 30/07/2015 20:02:14.

including a human protein involved in fatty acid biosynthesis (~50 kDa) and several proteins provided by ATCG3D, were screened in this manner. Crystals were already obtained from one of these proteins. Further optimization of these crystallization conditions is currently underway using previously described procedures.[5] We believe that the technique we have analyzed in this paper is not limited to generating cartridges for screening of protein crystallization conditions, and would enhance and simplify chemical screening[3] and biological assays.[4]

Acknowledgements

This work was partially supported by the NIH (RO1 GM075827). We acknowledge ATCG3D, funded by the National Institute of General Medical Sciences and National Center for Research Resources under the PSI-2 Specialized Center program (U54 GM074961), for providing equipment. Undergraduate research was supported by Dreyfus Teacher-Scholar award to R. F. I. (D. A.) and by the NIH Roadmap Physical and Chemical Biology training program at the University of Chicago (D. M.). We thank the Haselkorn group at the University of Chicago and Peter Kuhn and Ray Stevens groups at the Scripps Research Institute for protein samples. Fluorescent measurements were performed at the Chicago MRSEC microfluidic facility funded by NSF. We thank Qiang Fu, Helen Song and Liang Li for helpful discussions.

References

1 D. C. Carter, P. Rhodes, D. E. McRee, L. W. Tari, D. R. Dougan, G. Snell, E. Abola and R. C. Stevens, *J. Appl. Crystallogr.*, 2005, **38**, 87–90.
2 V. Linder, S. K. Sia and G. M. Whitesides, *Anal. Chem.*, 2005, **77**, 64–71.
3 T. Hatakeyama, D. L. L. Chen and R. F. Ismagilov, *J. Am. Chem. Soc.*, 2006, **128**, 2518–2519.
4 B. Zheng and R. F. Ismagilov, *Angew. Chem., Int. Ed.*, 2005, **44**, 2520–2523.
5 B. Zheng, L. S. Roach and R. F. Ismagilov, *J. Am. Chem. Soc.*, 2003, **125**, 11170–11171.
6 T. A. Thorsen, *Biotechniques*, 2004, **36**, 197–199.
7 H. Song, J. D. Tice and R. F. Ismagilov, *Angew. Chem., Int. Ed.*, 2003, **42**, 768–772.
8 B. Zheng, J. D. Tice and R. F. Ismagilov, *Anal. Chem.*, 2004, **76**, 4977–4982.
9 D. R. Link, S. L. Anna, D. A. Weitz and H. A. Stone, *Phys. Rev. Lett.*, 2004, 92.
10 J. C. McDonald and G. M. Whitesides, *Acc. Chem. Res.*, 2002, **35**, 491–499.
11 D. C. Duffy, J. C. McDonald, O. J. A. Schueller and G. M. Whitesides, *Anal. Chem.*, 1998, **70**, 4974–4984.
12 L. S. Roach, H. Song and R. F. Ismagilov, *Anal. Chem.*, 2005, **77**, 785–796.
13 P. Gonzaleztello, F. Camacho and G. Blazquez, *J. Chem. Eng. Data*, 1994, **39**, 611–614.
14 R. K. Shah and A. L. London, *Laminar Flow Forced Convection in Ducts: a Source Book for Compact Heat Exchanger Analytical Data*, Academic Press, New York, 1978.
15 W. L. Olbricht and D. M. Kung, *Phys. Fluids A*, 1992, **4**, 1347–1354.
16 K. J. Stebe, S. Y. Lin and C. Maldarelli, *Phys. Fluids A*, 1991, **3**, 3–20.
17 M. J. Martinez and K. S. Udell, *J. Fluid Mech.*, 1990, **210**, 565–591.
18 A. Borhan and C. F. Mao, *Phys. Fluids A*, 1992, **4**, 2628–2640.
19 T. M. Tsai and M. J. Miksis, *J. Fluid Mech.*, 1994, **274**, 197–217.
20 P. Garstecki, M. J. Fuerstman, H. A. Stone and G. M. Whitesides, *Lab Chip*, 2006, **6**, 437–446.
21 M. A. Unger, H. P. Chou, T. Thorsen, A. Scherer and S. R. Quake, *Science*, 2000, **288**, 113–116.
22 D. B. Weibel, M. Kruithof, S. Potenta, S. K. Sia, A. Lee and G. M. Whitesides, *Anal. Chem.*, 2005, **77**, 4726–4733.
23 A. Gunther, M. Jhunjhunwala, M. Thalmann, M. A. Schmidt and K. F. Jensen, *Langmuir*, 2005, **21**, 1547–1555.
24 A. Gunther, S. A. Khan, M. Thalmann, F. Trachsel and K. F. Jensen, *Lab Chip*, 2004, **4**, 278–286.

 This journal is © The Royal Society of Chemistry 2006